BIOCHEMISTRY
including biophysical chemistry & molecular biology

Article

pubs.acs.org/biochemistry

Mechanism of Glutathione Transferase P1-1-Catalyzed Activation of the Prodrug Canfosfamide (TLK286, TELCYTA)

Daniel F. A. R. Dourado,[†,‡,§,∥] Pedro Alexandrino Fernandes,[†] Maria João Ramos,*[,†] and Bengt Mannervik[‡,§]

[†]REQUIMTE/Departamento de Química e Bioquímica, Faculdade de Ciências, Universidade do Porto, Rua do Campo Alegre s/n, 4169-007 Porto, Portugal

[‡]Department of Chemistry-BMC, Uppsala University, Box 576, SE-75123 Uppsala, Sweden

[§]Department of Neurochemistry, Stockholm University, SE-10691 Stockholm, Sweden

Supporting Information

ABSTRACT: Canfosfamide (TLK286, TELCYTA) is a prodrug that upon activation by glutathione transferase P1-1 (GST P1-1) yields an anticancer alkylating agent and a glutathione derivative. The rationale underlying the use of TLK286 in chemotherapy is that tumor cells overexpressing GST P1-1 will be locally exposed to the released alkylating agent with limited collateral toxicity to the surrounding normal tissues. TLK286 has demonstrated clinical effects in phase II and III clinical trials for the treatment of malignancies, such as ovarian cancer, nonsmall cell lung cancer, and breast cancer, as a single agent and in combination with other chemotherapeutic agents. In spite of these promising results, the detailed mechanism of GST P1-1 activation of the prodrug has not been elucidated. Here, we propose a mechanism for the TLK286 activation by GST P1-1 on the basis of density functional theory (DFT) and on potential of mean force (PMF) calculations. A catalytic water molecule is instrumental to the activation by forming a network of intermolecular interactions between the active-site Tyr7 hydroxyl and the sulfone and COO^- groups of TLK286. The results obtained are consistent with the available experimental kinetic data and provide an atomistic understanding of the TLK286 activation mechanism.

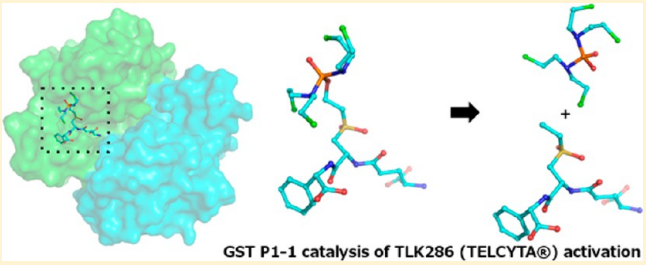

Glutathione transferase P1-1 (GST P1-1) is overexpressed in many tumor cells[1−3] and has been implicated in the development of anticancer drug resistance.[4−11] Canfosfamide (TLK286, TELCYTA) is a glutathione analogue prodrug that is activated by GST P1-1[12,13] (Figure 1). The rationale for the use of TLK286 is the high expression level of the enzyme in tumor cells, which is expected to focus the release of the active drug to the malignant target tissues, thus limiting significant collateral toxicity. In vitro studies, using tumor cell lines and even drug-resistant tumor cell lines, demonstrated that when GST P1-1 is overexpressed TLK286 shows strong antitumor activity.[14] In vivo analysis using xenograft models in nude mice led to similar conclusions and demonstrated that treatment with TLK286 causes only mild bone marrow toxicity as a side-effect.[14] These promising results have enabled several clinical trials in which the prodrug was used as a single agent or in combination with established chemotherapeutics. Phase II and III trials were performed for the treatment of malignancies such as ovarian cancer, nonsmall cell lung cancer, and breast cancer.[15−21] Overall, the clinical trials have identified TLK286 as a promising chemotherapeutic agent.

The mechanism of TLK286 activation by GST P1-1 involves the cleavage of the prodrug into a glutathione derivative and a phosphorodiamidate, of which the latter spontaneously forms alkylating aziridinium ring structures[12,13] (Figure 1). The glutathione derivative could act as a competitive inhibitor, counteracting the anticancer drug resistance promoted by GST P1-1. The aziridinium species, the actual alkylating agent, induces stress-mediated cellular apoptosis, possibly through activation of mitogen-activated protein (MAP) kinase, MKK4, jun-N-terminal kinase (JNK), p38 kinase, and caspase.[22] In addition, it can inhibit DNA-dependent protein kinase (DNA-PK), which is associated with the nonhomologous end-joining DNA repair and is required for the variable (V), diversity (D), and joining (J) gene recombination process.[23]

To date, no studies have been performed with the goal of understanding the detailed mechanism of TLK286 activation by GST P1-1. At the time when TLK286 was designed, the GSH activation in the conventional reactions was poorly understood. A possibility was that the phenolate of the Tyr7 side chain could work as a base, abstracting the proton from the GSH thiol group.[12,13] By analogy, it was suggested that Tyr7 could deprotonate the α-C methylene group of TLK286 (see atoms nomenclature in Figure 1). Then, the phosphorodiamidate, bound to the adjacent β-C, would be released in a β-elimination reaction to

Received: May 5, 2013
Revised: September 5, 2013
Published: September 25, 2013

ACS Publications © 2013 American Chemical Society

dx.doi.org/10.1021/bi4005705 | *Biochemistry* 2013, 52, 8069−8078

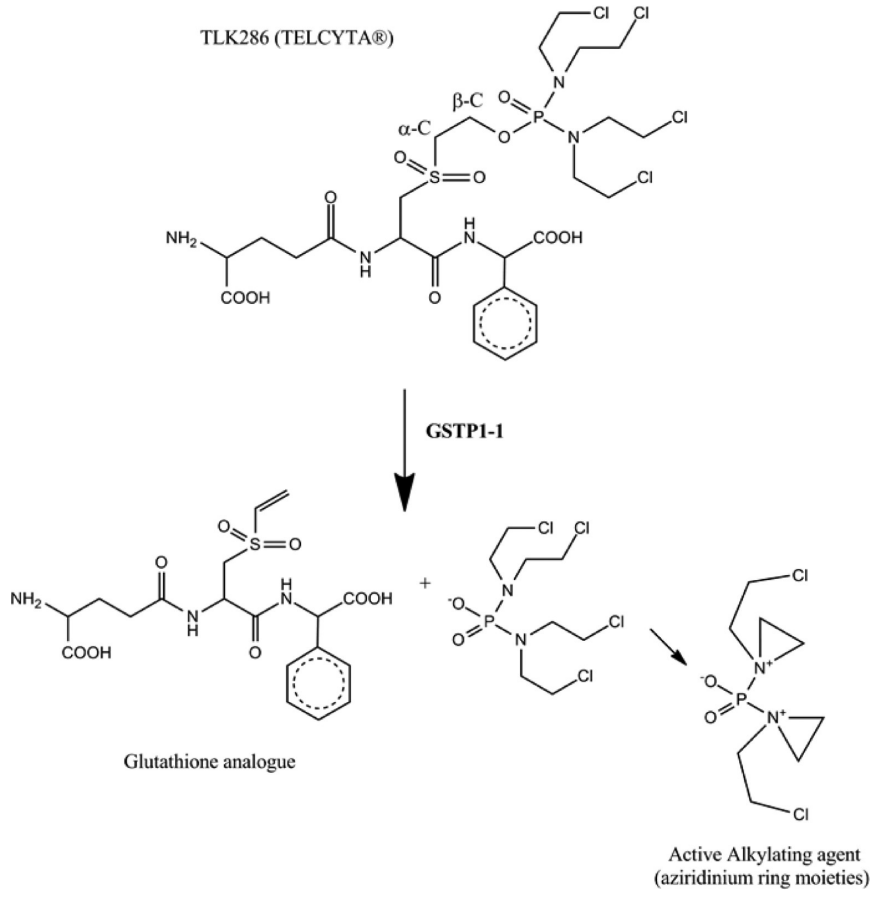

Figure 1. General scheme for the activation of TLK286 by GST P1-1.

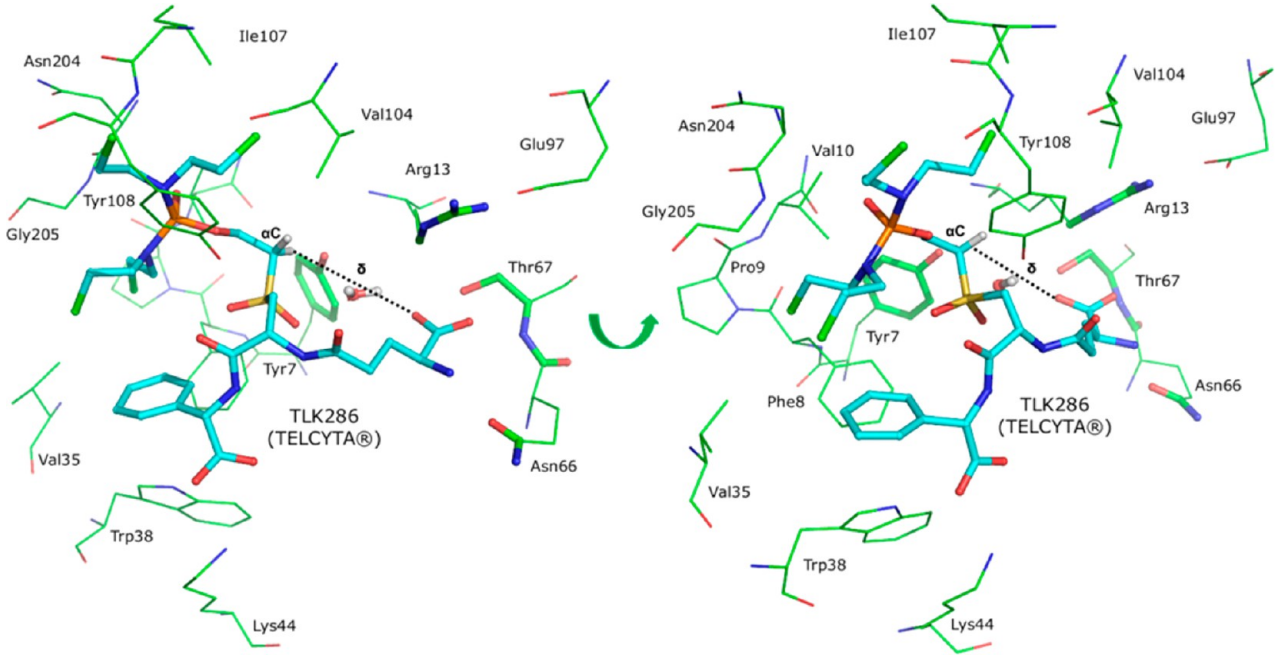

Figure 2. Model of the G- and H-site pockets (387 atoms) in two different orientations. The high layer (124 atoms) is represented by sticks, and the low layer is represented by lines. Also shown are the α-C hydrogen atom (A) and the carboxylate oxygen (B), which define the distance, δ, taken as the reaction coordinate in the PMF calculation. The hydrogen atoms are omitted except for those of the TLK286 α-C and water molecules.

form a double bond between the α-C and β-C.[12,13] However, it was demonstrated that this conserved Tyr is not a good base because its side-chain pK_a is considerably higher than the optimal pH value for GSTs activity (~7.4).[24] Instead, computational studies have identified a water molecule coupled with the α-carboxylate of the glutamyl group of GSH itself as the base

dx.doi.org/10.1021/bi4005705 | *Biochemistry* 2013, 52, 8069−8078

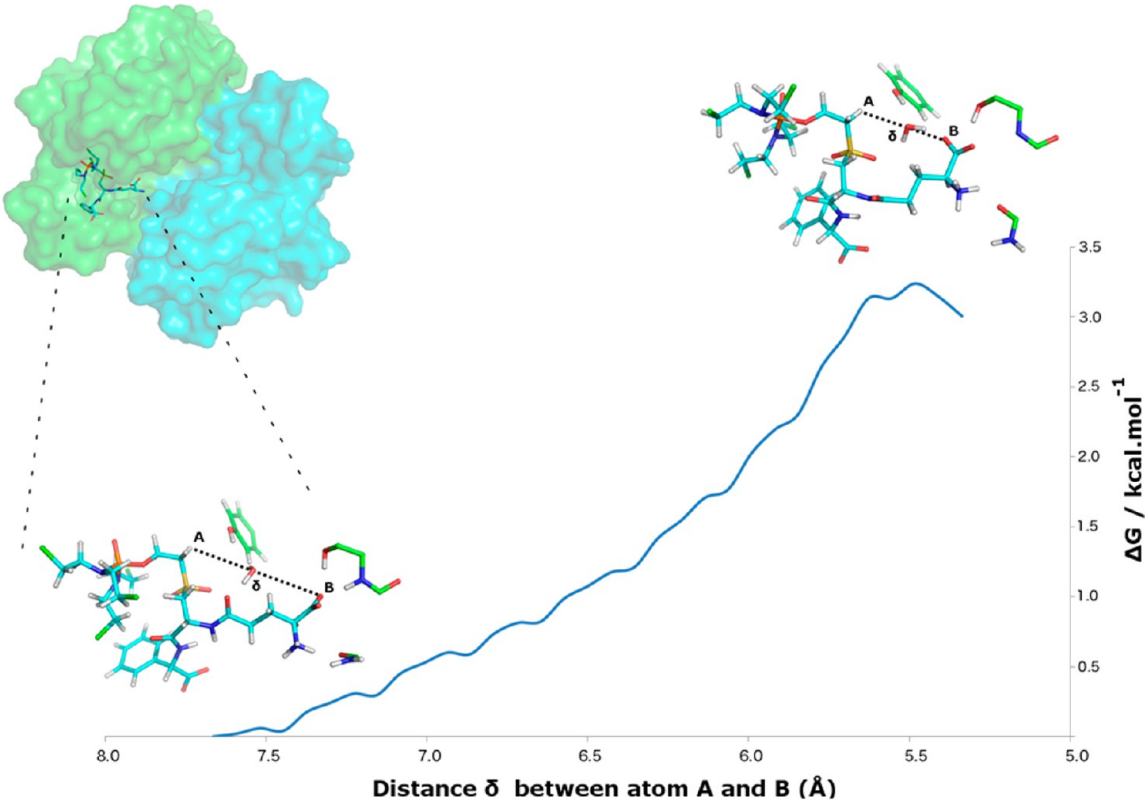

Figure 3. TLK286 structural rearrangement. The curve represents the sum of the entire data obtained from the PMF forward and backward processes. Initial and final TLK286 structures from GST P1-1 are shown. The reaction coordinate δ between atoms A (α-C hydrogen atom) and B (carboxylate oxygen) is indicated by a dotted line.

responsible for GSH activation in GST P1-1 and the other GSTs studied.[25−27]

On the basis of our model of GSH activation, we hypothesized that a water molecule could similarly mediate a proton transfer from the α-C to the α-carboxylate of TLK286 (TLK286 COO^-) (Figure 2). Subsequently, the phosphorodiamidate would be released and a double bond formed between α-C and β-C. We tested this proposal as well as other hypotheses that emerged while the work was being conducted, resorting to density functional theory (DFT) and potential of mean force (PMF) calculations.

METHODS

Molecular Dynamics of TLK286 Conformational Change. The crystal structure of GST P1-1 complexed with the GSH-electrophile (9*R*,10*R*)-9-(*S*-glutathionyl)-10-hydroxy-9,10-dihydrophenanthrene (GPR)[28] was used to model TLK286 within the G- and H-site pockets. Both GPR and TLK286 have a GSH moiety in their core structure, so both should share an identical G-site fit. The GPR dihydrophenanthrene ring and the TLK286 phosphorodiamidate have a comparable size and shape, which suggests that the initial fit of TLK286 phosphorodiamidate in the H-site can be derived from the GPR structure. To our knowledge, no other GST P1-1 crystal structure exhibiting a ligand with such molecular characteristics is available. The GPR dihydrophenanthrene ring was transformed into the TLK286 phosphorodiamidate using the Accelrys Discovery Studio software.[29] TLK286 had to be parametrized because there are no parameters describing the structure in the PARM99 force field.[30,31] The sulfone group dihedrals, angles, bonds, and van der Waals parameters were based on a paper by Altona et al.[32] The missing parameters for the phosphate group were obtained with GAFF (general AMBER force field).[31] The parameters for the remainder of the molecule were based on the PARM99 force field. Atomic point charges were calculated with the GAUSSIAN software package following the methodology used in the AMBER99 force field by fitting the HF/6-31G* generated electrostatic potential to atomic point charges using the RESP algorithm.

After obtaining the parameters for TLK286, the enzyme model was solvated with ∼16 000 single-point-charge waters (SPC)[33] and then submitted to 100 steps of steepest-descent energy minimization to remove poor contacts between the solvent and the protein. Subsequently, the system was equilibrated with a 200 ps molecular dynamics (MD) simulation, maintaining the protein atoms restrained by weak harmonic constraints to allow for the structural relaxation of the water molecules. Subsequently, an MD production simulation of 50 ns was performed to relax the prodrug structure within the G- and H-site pockets. A time step of 0.002 ps was applied, and the trajectories were saved at every 1 ps. A reference structure of this production simulation, which corresponds to the structure that is more similar to the average structure, was used as the starting point for the PMF calculations. A water molecule was later added and placed between the TLK286 α-C and TLK286 COO^- (Figure 2). All of the details of the PMF calculation will be described in a subsequent section.

Periodic boundary conditions were used in all simulations. The temperature and pressure were maintained constant using the Berendsen temperature coupling and pressure coupling (parameters: τ_T = 0.1 ps, T_{ref} = 300 K, and P_{ref} =1 bar).[34] The particle mesh Ewald (PME)[35] method was applied to compute

dx.doi.org/10.1021/bi4005705 | *Biochemistry* 2013, 52, 8069−8078

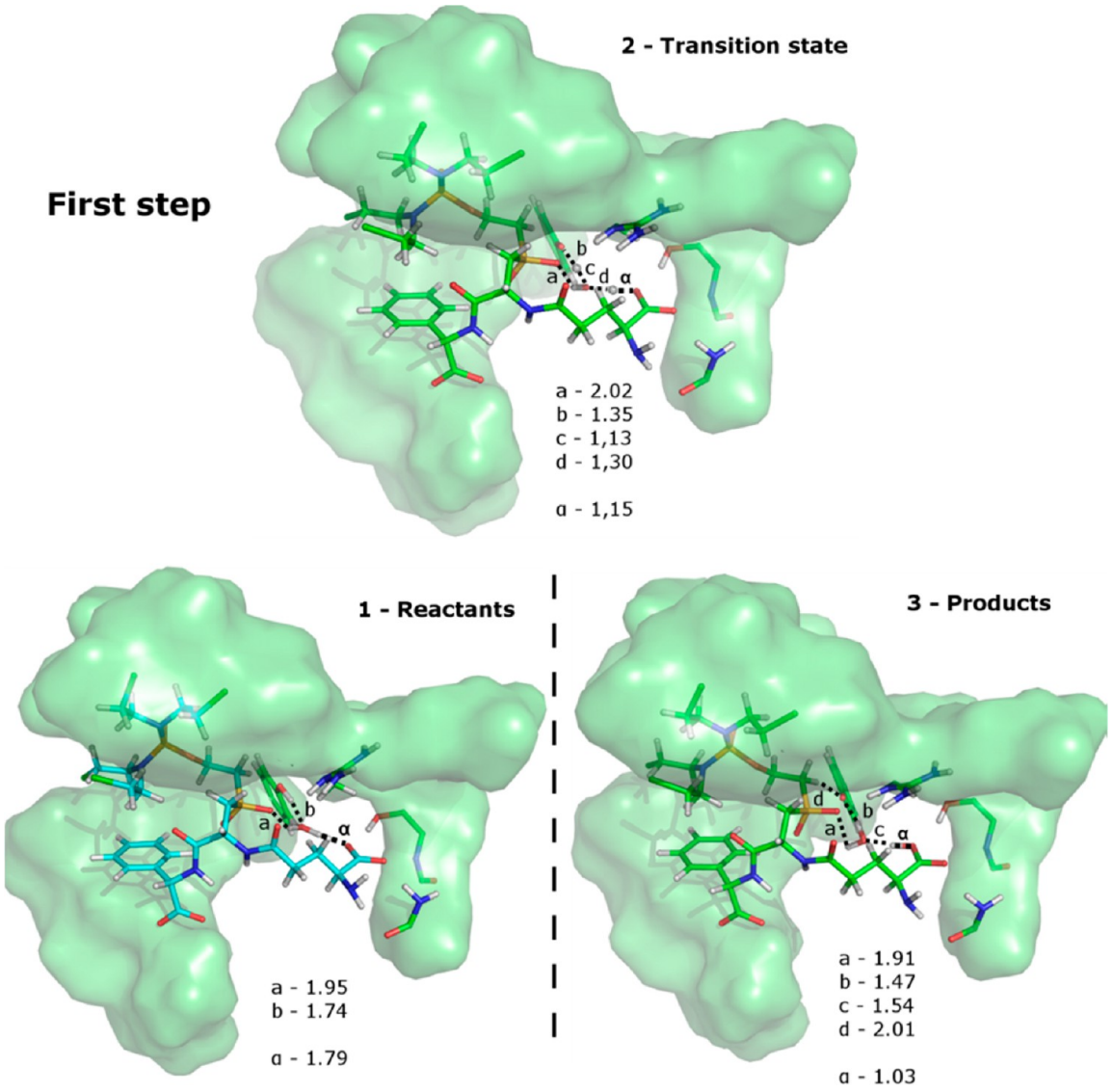

Figure 4. First step of the TLK286 activation by GST P1-1. The reaction coordinate (α) corresponds to the distance between a water-molecule proton and the TLK286 COO^- oxygen atom. Relevant distances (Å) are shown.

electrostatic interactions with a cutoff of 1.0 nm. A twin range cutoff with a neighbor list cutoff of 1.0 and a van der Waals cutoff of 1.0 was used for the van der Waals interactions. All of the bonds involving hydrogen atoms were constrained by the LINCS constraint algorithm.[36] All of the simulations and subsequent analyses were carried out using the Gromacs software package in conjunction with the Amber99 force field.[30,31,37,38]

Potential of Mean Force Calculations. A potential of mean force (PMF) represents the Gibbs free-energy change as a function of a coordinate of the system. The PMF calculation was performed with the umbrella sampling method.[39] In the umbrella sampling method, a series of simulations windows are performed along a reaction coordinate, and each window is restrained by imposing a harmonic umbrella biased potential $U'(\delta)$

$$U'(\delta) = 1/2\kappa(\delta - \delta_0)^2$$

where κ is the force constant. In our study, the distance δ between the hydrogen (atom A) of α-C and the proximal oxygen (atom B) of TLK286 COO^- was taken as the reaction coordinate (Figure 2). This distance was steadily decreased in each window by 0.04 Å. The backwards process was also performed starting from the last structure of the preceding process. The force constant was calibrated to allow an overlapping of the windows along the reaction coordinate (K = 50−150 kcal mol^{-1}). A total of eight forward and eight backward 200 ps windows were performed, resulting in 3200 ps production simulations overall. The unbiased probability distribution of δ values, in both the forward and backward directions, was used to calculate the free energy associated with the approach of the TLK286 α-C to the TLK286 COO^- by the constant temperature-weighted histogram-analysis method (WHAM).[40] The WHAM method allows for the calculation of the PMF by computing the unbiased distribution function as a weighted sum over the individual biased distributions of each window.

Proton Transfer from α-C to COO^- in TLK286. A model of the G- and H-site pockets (387 atoms) was built from a final PMF structure (Figure 2).

This model includes TLK286 and all of the residues considered important to catalysis (Tyr7, Phe8, Pro9, Val10, Arg13, Val35, Trp38, Lys44, Asn66, Thr67, Glu97, Val104, Ile107, Asp204, and Gly205). The main chain of the residues was kept neutral by introducing hydrogen atoms as link atoms at the

dx.doi.org/10.1021/bi4005705 | *Biochemistry* 2013, 52, 8069−8078

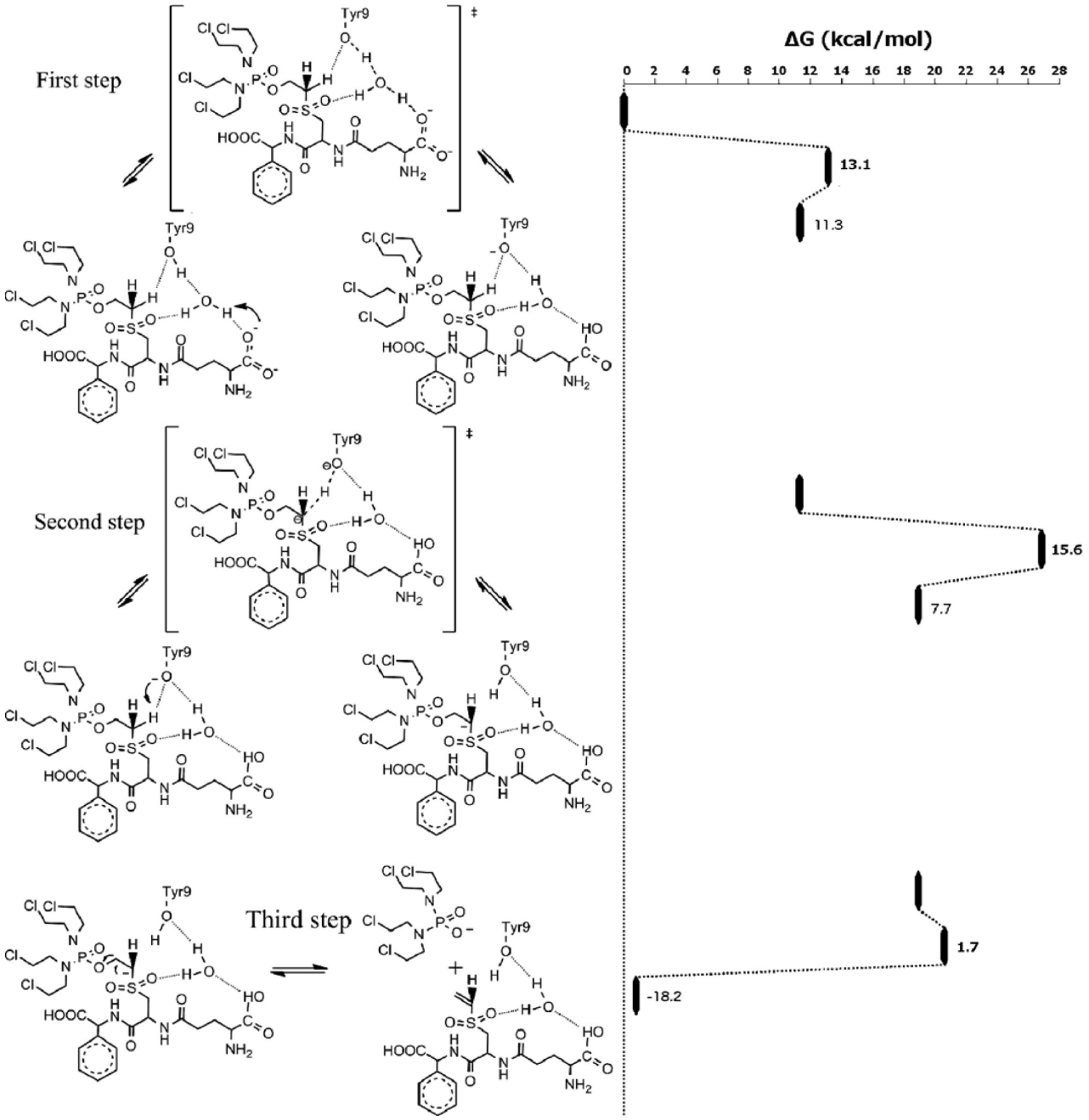

Figure 5. Free-energy barriers of TLK286 activation by GST P1-1. The full mechanism is composed of the three catalytic steps described in the text.

truncated bonds. All α carbons were kept fixed during the study to avoid possible local unfolding. The geometry optimizations were conducted with the ONIOM hybrid method,[41−43] as implemented in Gaussian 09.[44] In geometry optimizations, the high layer was described with DFT using the B3LYP functional and the 6-31G(d) basis set.[45,46] It includes TLK286 and atoms from residues Tyr7, Arg13, Asn66, and Thr67 in a total of 124 atoms, as demonstrated in Figure 2. The low layer was treated with the semiempirical method PM3MM.[47,48] It includes residues Phe8, Pro9, Val10, Val35, Trp38, Lys44, Glu97, Val104, Ile107, Asp204, and Gly205 as well as the atoms of residues Tyr7, Arg13, Asn66, and Thr67 that were not included in the high layer (Figure 2).

First, we conducted a linear scan of the water proton approach to the most suitable TLK286 COO^- oxygen atom. The results led to a reformulation of the initial proposal for the TLK286 activation. A full description follows in the next section. In accordance, we performed a linear scan of the TLK286 α-C proton transfer to the Tyr7 side chain and also a linear scan of the TLK286 β-C and adjacent oxygen bond stretching. Initial guesses for the structures of the stationary points (reagent, transition state, and product) were taken from all of the scans. The stationary points were later optimized, and their nature was confirmed by frequency calculations. After obtaining the three stationary points, we performed single point calculations to obtain the energy of the high layer at the B3LYP/6-311++G(2d,2p) level. A continuum model was used as an approximation to the effect of the protein beyond the atomistic region. We chose the ONIOM-PCM continuum model,[49,50] as implemented in G09, with a dielectric constant of 4. Zero point

dx.doi.org/10.1021/bi4005705 | *Biochemistry* 2013, 52, 8069−8078

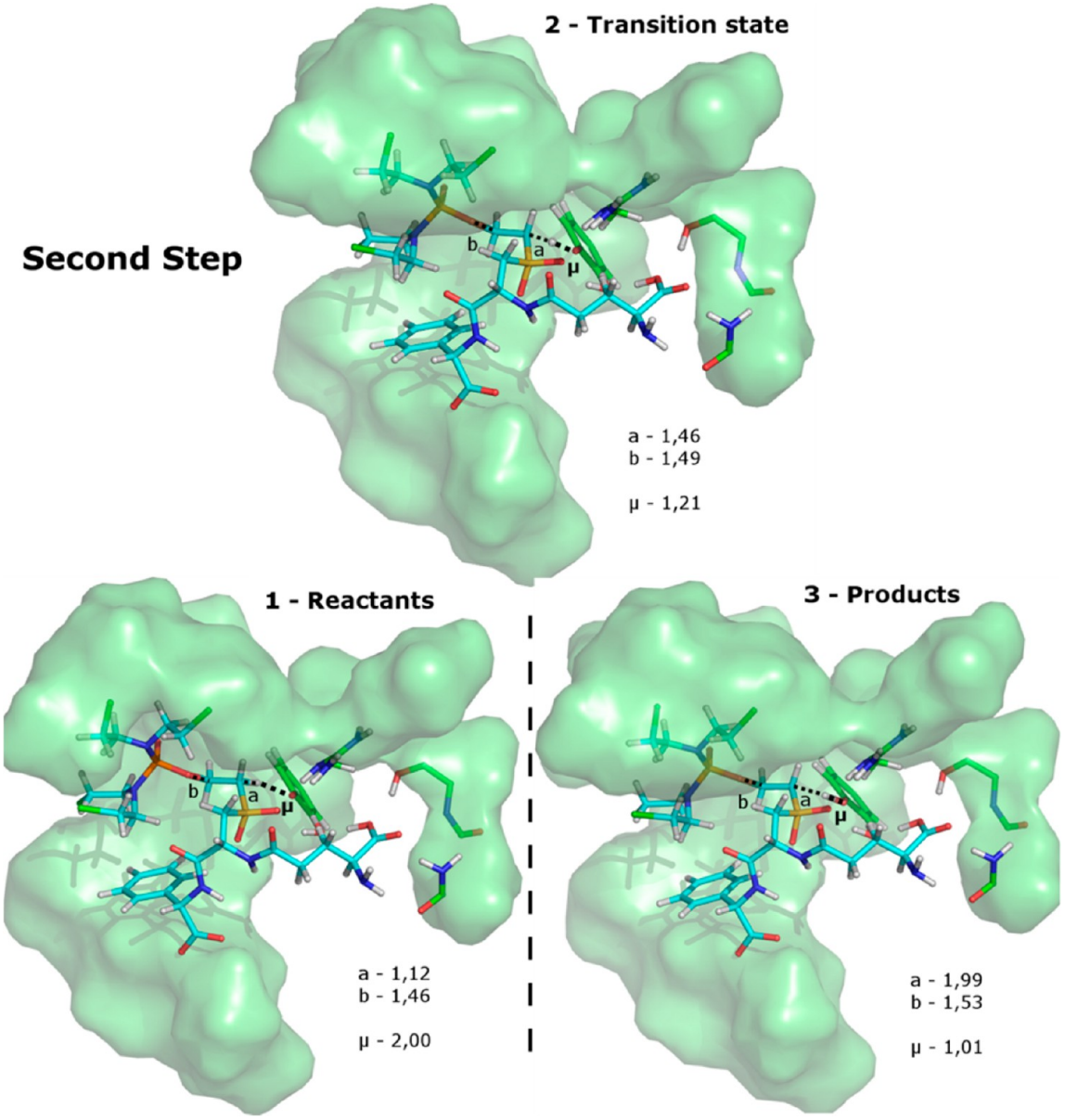

Figure 6. Second step of the TLK286 activation by GST P1-1. The reaction coordinate (μ) corresponds to the distance between the TLK286 α-C proton and the Tyr7 side-chain oxygen atom. Relevant distances (Å) are shown.

corrections as well as thermal and entropic effects were also added to obtain the final free-energy values (T = 310.15 K and P = 1 bar). This methodology has recently been used with excellent results in the study of several enzyme mechanisms.[26,27,51−58]

RESULTS AND DISCUSSION

Water-Assisted TLK286 Activation Mechanism. We began by testing the hypothesis that a water molecule is able to bridge a proton transfer between the TLK286 α-C and the TLK286 COO^-. First, we calculated the free-energy barrier associated with the TLK286 conformational rearrangement from an opened extended conformation to a closed conformation. For this purpose, we calculated the corresponding potential of mean force (PMF) using the umbrella sampling method. Subsequently, a model of the G- and H-site pockets was built starting from the final PMF structure and was described at the DFT level. We then performed the necessary linear scans for the relevant reaction coordinates. From the scans, the structures of the stationary points were obtained, and the respective energies were calculated.

The results dictated a reformulation of our initial proposal. The full description of the used methodology follows.

TLK286 Conformational Rearrangement. Figure 3 shows the free-energy barrier involved in the TLK286 structural rearrangement.

The PMF curve shown reflects the sum of the forward and backward processes. By comparing the forward and backward PMF curves, we observe only minimal hysteresis, rejecting the possibility of systematic error and emphasizing the accuracy of the calculations.

As in the GSH activation,[27] the open conformation of TLK286 is more stable. The free-energy barrier, 3.24 kcal mol^{-1}, is higher than the one observed in the GSH rearrangement, 1.92 kcal mol^{-1},[27] which can be expected because of the steric hindrance associated with moving the phosphorodiamidate portion of TLK286 .

dx.doi.org/10.1021/bi4005705 | *Biochemistry* 2013, 52, 8069−8078

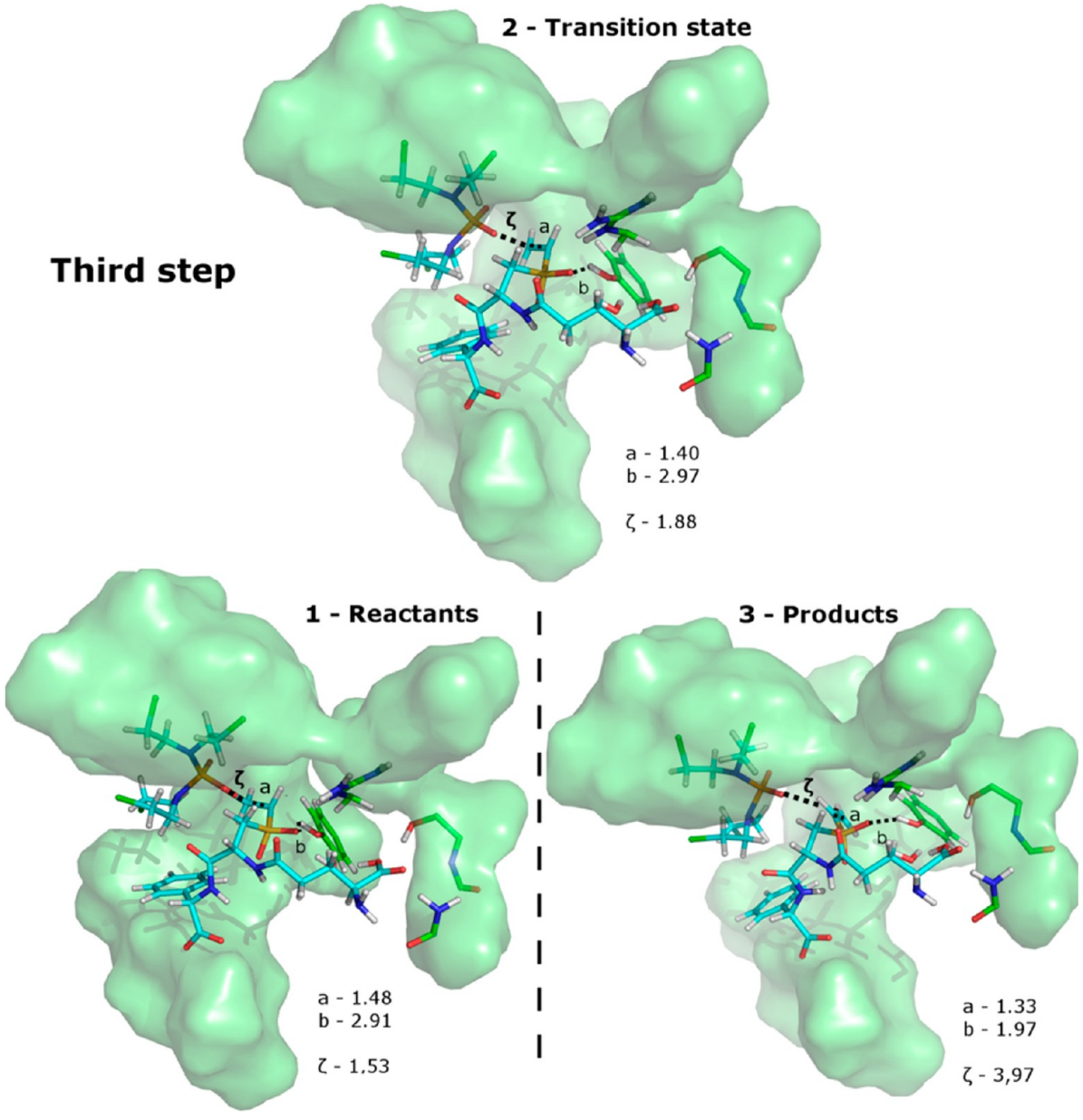

Figure 7. Third step of the TLK286 activation by GST P1-1. The reaction coordinate (ζ) corresponds to the distance between the TLK286 β-C and the adjacent oxygen. Relevant distances (Å) are shown.

Proton Transfer. Starting from the final structure of the PMF calculation, we built a model of the G- and H-site pockets (Figure 2). Then, we conducted a linear scan of the water proton approach to the most suitable TLK286 COO^- oxygen atom. We were expecting to see a simultaneous proton transfer from the α-C to the water molecule. However, that was not observed.

In the GSH activation, the residue Tyr7 is fundamental to stabilizing the charge that is formed in the ionization of the thiol group.[27] When the TLK286 prodrug substitutes for the substrate, Tyr7 does not have this role and assumes a somewhat different orientation in the active center, being hydrogen bonded to the water molecule (Figure 4.1b). The water molecule is also simultaneously interacting with the TLK286 sulfone group (Figure 4.1a).

When we transfer the proton from the water molecule to the TLK286 COO^- oxygen atom (Figure 4, α), the Tyr 7 hydroxyl transfers a proton to the water molecule, as the transition-state structure shows (Figure 4.2). In the product structure, the Tyr7 side chain establishes an ionic hydrogen bond with the water molecule (Figure 4.3-b) and simultaneously acts as a base, receiving a proton from the α-C (Figure 4.3d). Additionally, the hydrogen bond between the water molecule and the TLK286 sulfone group becomes stronger (Figure 4.a). This reaction has an activation energy ($\Delta G^{\ddagger}$) of 13.1 kcal mol^{-1} and a reaction free energy (ΔG_r) of 11.3 kcal mol^{-1} (Figure 5).

At this point it became clear that our initial proposal needed reformulation and definitely needed to include Tyr 7 as a fundamental residue to catalysis.

In the second step of our mechanism, Tyr7 works as a base and receives the proton from the TLK286 α-C carbon atom (Figure 6).

As we transfer the proton, the bond between the β-C carbon atom and the adjacent oxygen of the phosphorodiamidate becomes weaker (Figure 6.b), but it does not break. This step has

dx.doi.org/10.1021/bi4005705 | *Biochemistry* 2013, 52, 8069−8078

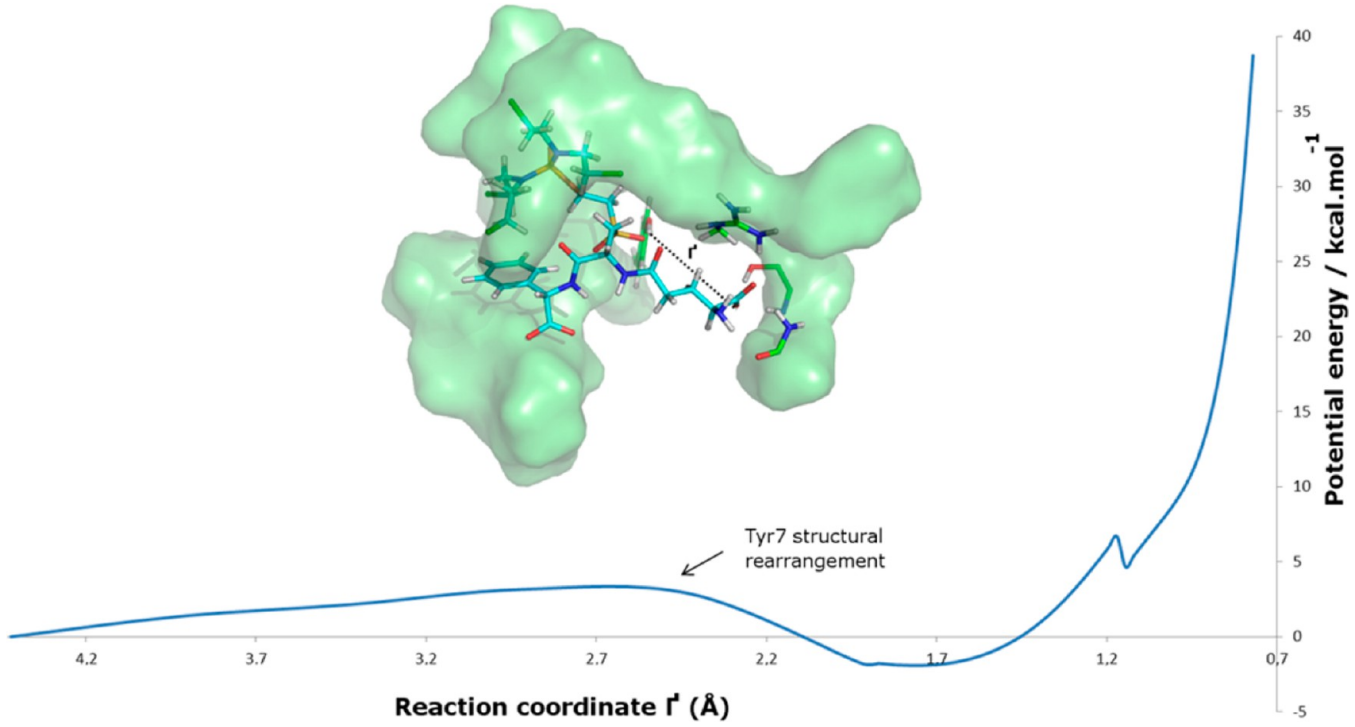

Figure 8. Potential-energy surface of the hypothetical proton transfer between the Tyr7 hydroxyl group and TLK286 COO^- oxygen atom. The reaction coordinate is indicated.

an activation energy ($\Delta G^{\ddagger}$) of 15.6 kcal mol^{-1} and a reaction free energy (ΔG_r) of 7.7 kcal mol^{-1} (Figure 5).

In the third step, we force the bond between the β-C carbon atom and the adjacent oxygen to break, observing the consequent release of the phosphorodiamidate (Figure 7).

The release of the phosphorodiamidate leads to the formation of a double bond between the α-C and the β-C atoms. Therefore, the distance between these atoms decreases from reactants to products (Figure 7.1a, 7.2a, and 7.3a).

The third step of the reaction has a low activation energy ($\Delta G^{\ddagger}$) of just 1.7 kcal mol^{-1} (Figure 5). A strong hydrogen bond between the Tyr 7 hydroxyl and the sulfone group (Figure 7.3b) greatly contributes to the stabilization of the product structure. We obtained a reaction free energy (ΔG_r) of −18.2 kcal mol^{-1} (Figure 5).

Importance of the Water Molecule to Catalysis. We performed a direct proton transfer between the Tyr 7 hydroxyl and the TLK286 COO^- oxygen atom to further elucidate the role of the water molecule. The model of the G- and H-site pockets can be seen in the Supporting Information (Figure S1). The linear scan identifies an initial structural rearrangement of the Tyr7 side chain with a barrier of 3.1 kcal mol^{-1} . However, we did not observe any stationary structures for this proton transfer (Figure 8). Without the water molecule, the reaction does not take place.

CONCLUSIONS

The TLK286 activation catalyzed by GST P1-1 was analyzed on the basis of alternative models. We began by testing the possibility of a water molecule being able to directly transfer a proton between the TLK286 α-C atom and the TLK286 COO^- group. This reaction model mimics the GSH activation mechanism observed in GST P1-1.[27] The results obtained were unrealistic and necessitated a reformulation of the initial proposal. The new mechanism proposal can be divided into three catalytic steps. In the first step, a water molecule transfers a proton between the Tyr7 hydroxyl and the TLK286 COO^- oxygen atom. In the second step, Tyr7 works as a base and receives a proton from TLK286 α-C atom. In the third step, we observe the breaking of the bond between TLK286 β-C and the adjacent oxygen and the consequent release of the phosphorodiamidate. The water molecule provides a network of intermolecular interactions between the Tyr7 hydroxyl and the TLK286 sulfone and COO^- groups, which is essential to maintain an effective charge distribution in the different steps of the mechanism. Obviously, the water molecule plays a pivotal role in the reaction.

The rate-determining states of the whole cycle are the transition state of the second step and the reactant of the first step, leading to an energetic span of 26.8 kcal mol^{-1}. The experimentally determined half-life of TLK286 activation by GST P1-1 is ∼1 h.[12,13] Considering that the half-life of a first-order reaction is independent of the starting concentration and is given by ln2 over the rate of reaction, the energy span of this reaction can be estimated at 23 kcal mol^{-1}. This value is not significantly different from our calculated value of 26.8 kcal mol^{-1} considering the error associated with both experiments and calculation. The good agreement between the energy values strongly indicate that the proposed mechanism is plausible and realistic.

For comparison, the GSH activation by GST P1-1 has an energetic span of 11.4 kcal mol^{-1},[27] which is considerably lower than the high energy barrier of TLK286 activation by GST P1-1. The TLK286 activation barrier may be thought as high for an enzymatic reaction. However, we should take into account that TLK286 is not a natural substrate, and it is clear that its activation catalyzed by GST P1-1 is many orders of magnitude slower[12,13] than the conjugation of GSH with standard substrates.[24] As described above, when TLK286 was designed, it was believed

dx.doi.org/10.1021/bi4005705 | *Biochemistry* 2013, 52, 8069−8078

that Tyr7 would also easily deprotonate the TLK286 α-C.[59] However, a later study[24] demonstrated that Tyr7 is a weak base because the pK_a of its side chain is substantially higher than the pH associated with GSTs catalysis, and this present work provides atomic-level evidence of this.

The computational methods employed demonstrated results in accordance with the experimental data, indicating that new modifications to the prodrug can be evaluated in silico with high cost-effectiveness prior to conducting any in vitro or in vivo studies.

■ ASSOCIATED CONTENT

Supporting Information

Model of the G- and H-site pockets without the catalytic water (384 atoms). This material is available free of charge via the Internet at http://pubs.acs.org.

■ AUTHOR INFORMATION

Corresponding Author

*E-mail: mjramos@fc.up.pt. Tel.: +351 220 402 506.

Present Address

[‖]Department of Cell and Molecular Biology, Computational and Systems Biology, Uppsala Biomedicinska Centrum BMC, Box 596 751 24, Uppsala, Sweden.

Funding

We thank the FCT (Fundação para a Ciência e Tecnologia) for financial support (project POCI/QUI/61563/2004) as well as for Postdoctoral grant SFRH/BPD/74441/2010 for D.F.A.R.D. B.M. was supported by the Swedish Research Council and the Swedish Cancer Society.

Notes

The authors declare no competing financial interest.

■ REFERENCES

(1) Castro, V. M., Soderstrom, M., Carlberg, I., Widersten, M., Platz, A., and Mannervik, B. (1990) Differences among human tumor cell lines in the expression of glutathione transferases and other glutathione-linked enzymes. *Carcinogenesis 11*, 1569−1576.

(2) Mannervik, B., Castro, V. M., Danielson, U. H., Tahir, M. K., Hansson, J., and Ringborg, U. (1987) Expression of class Pi glutathione transferase in human malignant melanoma cells. *Carcinogenesis 8*, 1929−1932.

(3) Sugioka, Y., Fujii-Kuriyama, Y., Kitagawa, T., and Muramatsu, M. (1985) Changes in polypeptide pattern of rat liver cells during chemical hepatocarcinogenesis. *Cancer Res. 45*, 365−378.

(4) Tsuchida, S., and Sato, K. (1992) Glutathione transferases and cancer. *Crit. Rev. Biochem. Mol. Biol. 27*, 337−384.

(5) Raha, A., and Tew, K. D. (1996) Glutathione S-transferases. *Cancer Treat. Res. 87*, 83−122.

(6) Waxman, D. J. (1990) Glutathione S-transferases: Role in alkylating agent resistance and possible target for modulation chemotherapy−a review. *Cancer Res. 50*, 6449−6454.

(7) Tew, K. D. (1994) Glutathione-associated enzymes in anticancer drug resistance. *Cancer Res. 54*, 4313−4320.

(8) Niitsu, Y., Takahashi, Y., Ban, N., Takayama, T., Saito, T., Katahira, T., Umetsu, Y., Nakajima, T., Ohi, M., Kuga, T., Sakamaki, S., Matsunaga, T., Hirayama, Y., Kuroda, H., Homma, H., Kato, J., and Kogawa, K. (1998) A proof of glutathione S-transferase-pi-related multidrug resistance by transfer of antisense gene to cancer cells and sense gene to bone marrow stem cell. *Chem.−Biol. Interact. 111−112*, 325−332.

(9) Lewis, A. D., Hayes, J. D., and Wolf, C. R. (1988) Glutathione and glutathione-dependent enzymes in ovarian adenocarcinoma cell lines derived from a patient before and after the onset of drug resistance: Intrinsic differences and cell cycle effects. *Carcinogenesis 9*, 1283−1287.

(10) Kuzmich, S., Vanderveer, L. A., Walsh, E. S., LaCreta, F. P., and Tew, K. D. (1992) Increased levels of glutathione S-transferase pi transcript as a mechanism of resistance to ethacrynic acid. *Biochem. J. 281*, 219−224.

(11) Letourneau, S., Greenbaum, M., and Cournoyer, D. (1996) Retrovirus-mediated gene transfer of rat glutathione S-transferase Yc confers in vitro resistance to alkylating agents in human leukemia cells and in clonogenic mouse hematopoietic progenitor cells. *Hum. Gene Ther. 7*, 831−840.

(12) Lyttle, M. H., Satyam, A., Hocker, M. D., Bauer, K. E., Caldwell, C. G., Hui, H. C., Morgan, A. S., Mergia, A., and Kauvar, L. M. (1994) Glutathione-S-transferase activates novel alkylating agents. *J. Med. Chem. 37*, 1501−1507.

(13) Satyam, A., Hocker, M. D., Kane-Maguire, K. A., Morgan, A. S., Villar, H. O., and Lyttle, M. H. (1996) Design, synthesis, and evaluation of latent alkylating agents activated by glutathione S-transferase. *J. Med. Chem. 39*, 1736−1747.

(14) Morgan, A. S., Sanderson, P. E., Borch, R. F., Tew, K. D., Niitsu, Y., Takayama, T., Von Hoff, D. D., Izbicka, E., Mangold, G., Paul, C., Broberg, U., Mannervik, B., Henner, W. D., and Kauvar, L. M. (1998) Tumor efficacy and bone marrow-sparing properties of TER286, a cytotoxin activated by glutathione S-transferase. *Cancer Res. 58*, 2568−2575.

(15) Rosen, L. S., Brown, J., Laxa, B., Boulos, L., Reiswig, L., Henner, W. D., Lum, R. T., Schow, S. R., Maack, C. A., Keck, J. G., Mascavage, J. C., Dombroski, J. A., Gomez, R. F., and Brown, G. L. (2003) Phase I study of TLK286 (glutathione S-transferase P1-1 activated glutathione analogue) in advanced refractory solid malignancies. *Clin. Cancer Res. 9*, 1628−1638.

(16) Rosen, L. S., Laxa, B., Boulos, L., Wiggins, L., Keck, J. G., Jameson, A. J., Parra, R., Patel, K., and Brown, G. L. (2004) Phase 1 study of TLK286 (Telcyta) administered weekly in advanced malignancies. *Clin. Cancer Res. 10*, 3689−3698.

(17) Vergote, I., Finkler, N., del Campo, J., Lohr, A., Hunter, J., Matei, D., Kavanagh, J., Vermorken, J. B., Meng, L., Jones, M., Brown, G., and Kaye, S. (2009) Phase 3 randomised study of canfosfamide (Telcyta, TLK286) versus pegylated liposomal doxorubicin or topotecan as third-line therapy in patients with platinum-refractory or -resistant ovarian cancer. *Eur. J. Cancer 45*, 2324−2332.

(18) Sequist, L. V., Fidias, P. M., Temel, J. S., Kolevska, T., Rabin, M. S., Boccia, R. V., Burris, H. A., Belt, R. J., Huberman, M. S., Melnyk, O., Mills, G. M., Englund, C. W., Caldwell, D. C., Keck, J. G., Meng, L., Jones, M., Brown, G. L., Edelman, M. J., and Lynch, T. J. (2009) Phase 1−2a multicenter dose-ranging study of canfosfamide in combination with carboplatin and paclitaxel as first-line therapy for patients with advanced non-small cell lung cancer. *J. Thorac. Oncol. 4*, 1389−1396.

(19) Papadimitrakopoulou, V., Figlin, R., Garland, L., Von Hoff, D., Kris, M., Purdom, M., Brown, G. L., Maack, C., Macpherson, J., and Henner, W. D. (2002) Phase 2 study of TLK286 (GST P1-1 activated glutathione analog) in patients with non-small cell lung cancer who failed prior platinum-based regimens. *Eur. J. Cancer 38*, S36−S37.

(20) Kavanagh, J. J., Gershenson, D. M., Choi, H., Lewis, L., Patel, K., Brown, G. L., Garcia, A., and Spriggs, D. R. (2005) Multi-institutional phase 2 study of TLK286 (TELCYTA, a glutathione S-transferase P1-1 activated glutathione analog prodrug) in patients with platinum and paclitaxel refractory or resistant ovarian cancer. *Int. J. Gynecol. Cancer 15*, 593−600.

(21) Kavanagh, J. J., Levenback, C. F., Ramirez, P. T., Wolf, J. L., Moore, C. L., Jones, M. R., Meng, L., Brown, G. L., and Bast, R. C., Jr. (2010) Phase 2 study of canfosfamide in combination with pegylated liposomal doxorubicin in platinum and paclitaxel refractory or resistant epithelial ovarian cancer. *J. Hematol. Oncol. 3*, 9.

(22) Meng, F., Brown, G. L., Keck, J. G., Henner, W. D., Schow, S., Gomez, R. F., and Wick, M. M. (2001) TLK286-induced activation of JNK-dependent apoptotic signaling pathway. *Clin. Cancer Res. 7*, 3719s−3719s.

(23) Townsend, D. M., Shen, H. X., Staros, A. L., Gate, L., and Tew, K. D. (2002) Efficacy of a glutathione S-transferase pi-activated prodrug in platinum-resistant ovarian cancer. *Mol. Cancer Ther. 1*, 1089−1095.

(24) Björnestedt, R., Stenberg, G., Widersten, M., Board, P. G., Sinning, I., Jones, T. A., and Mannervik, B. (1995) Functional significance of arginine 15 in the active site of human class alpha glutathione transferase A1-1. *J. Mol. Biol. 247*, 765−773.
(25) Dourado, D. F. A. R., Fernandes, P. A., and Ramos, M. J. (2009) Glutathione transferase A1-1: Catalytic role of water. *Theor. Chem. Acc. 124*, 71−83.
(26) Dourado, D. F. A. R., Fernandes, P. A., Mannervik, B., and Ramos, M. J. (2008) Glutathione transferase: New model for glutathione activation. *Chem.—Eur. J. 14*, 9591−9598.
(27) Dourado, D. F., Fernandes, P. A., and Ramos, M. J. (2010) Glutathione transferase classes alpha, pi, and mu: GSH activation mechanism. *J. Phys. Chem. B 114*, 12972−12980.
(28) Ji, X. H., Tordova, M., ODonnell, R., Parsons, J. F., Hayden, J. B., Gilliland, G. L., and Zimniak, P. (1997) Structure and function of the xenobiotic substrate-binding site and location of a potential non-substrate-binding site in a class pi glutathione S-transferase. *Biochemistry 36*, 9690−9702.
(29) (2007) *Discovery Studio Modeling Environment, Release 2.1*, Accelrys Software Inc., San Diego, CA.
(30) Cornell, W. D., Cieplak, P., Bayly, C. I., Gould, I. R., Merz, K. M., Ferguson, D. M., Spellmeyer, D. C., Fox, T., Caldwell, J. W., and Kollman, P. A. (1995) A second generation force field for the simulation of proteins, nucleic acids, and organic molecules. *J. Am. Chem. Soc. 117*, 5179−5197.
(31) Wang, J., Wolf, R. M., Caldwell, J. W., Kollman, P. A., and Case, D. A. (2004) Development and testing of a general amber force field. *J. Comput. Chem. 25*, 1157−1174.
(32) Huige, C. J. M., and Altona, C. (1995) Force-field parameters for sulfates and sulfamates based on ab-initio calculations - extensions of amber and charmm fields. *J. Comput. Chem. 16*, 56−79.
(33) Berendsen, H., Postma, J. P. M., and vanGunsteren, W. F. (1981) *Intermolecular Forces*, D. Reidel Publishing Company, Dordrecht, The Netherlands.
(34) Berendsen, H., Postma, J. P. M., vanGunsteren, W. F., DiNola, A., and Haak., J. R. (1984) Molecular dynamics with coupling to an external bath. *J. Chem. Phys. 81*, 3584−3590.
(35) Essmann, U., Perera, L., Berkowitz, M. L., Darden, T., Lee, H., and Pedersen, L. G. (1995) A smooth particle mesh Ewald method. *J. Chem. Phys. 103*, 8577−8593.
(36) Hess, B., Bekker, H., Berendsen, H., and Fraaije., J. (1997) LINCS: A linear constraint solver for molecular simulations. *J. Comput. Chem. 18*, 1463−1472.
(37) Erik Lindahl, B. H., and van der Spoel, D. (2001) GROMACS 3.0: A package for molecular simulation and trajectory analysis. *J. Mol. Model. 7*, 306−317.
(38) Sorin, E. J., and Pande, V. S. (2005) Exploring the helix-coil transition via all-atom equilibrium ensemble simulations. *Biophys. J. 88*, 2472−2493.
(39) Torrie, G. M., and Valleau, J. P. (1977) Non-physical sampling distributions in monte-carlo free-energy estimation - umbrella sampling. *J. Comput. Phys. 23*, 187−199.
(40) Kumar, S., Bouzida, D., Swendsen, R. H., Kollman, P. A., and Rosenberg, J. M. (1992) The weighted histogram analysis method for free-energy calculations on biomolecules 0.1. The method. *J. Comput. Chem. 13*, 1011−1021.
(41) Bakowies, D., and Thiel, W. (1996) Hybrid models for combined quantum mechanical and molecular mechanical approaches. *J. Phys. Chem. 100*, 10580−10594.
(42) Dapprich, S., Komaromi, I., Byun, K. S., Morokuma, K., and Frisch, M. J. (1999) A new ONIOM implementation in Gaussian98. Part I. The calculation of energies, gradients, vibrational frequencies and electric field derivatives. *J. Mol. Struct.: THEOCHEM 462*, 1−21.
(43) Cosman, P. C., Rogers, J. K., Sherwood, P. G., and Zeger, K. (2000) Combined forward error control and packetized zerotree wavelet encoding for transmission of images over varying channels. *IEEE Trans. Image Process. 9*, 982−993.
(44) Frisch, M. J., et al. (2009) *Gaussian 09*, Gaussian, Inc., Wallingford, CT.
(45) Lee, C. T., Yang, W. T., and Parr, R. G. (1988) Development of the Colle-Salvetti correlation-energy formula into a functional of the electron-density. *Phys. Rev. B 37*, 785−789.
(46) Becke, A. D. (1993) Density-functional thermochemistry 0.3. The role of exact exchange. *J. Chem. Phys. 98*, 5648−5652.
(47) Stewart, J. J. P. (1989) Optimization of parameters for semiempirical methods 0.1. Method. *J. Comput. Chem. 10*, 209−220.
(48) Stewart, J. J. P. (1989) Optimization of parameters for semiempirical methods 0.2. Applications. *J. Comput. Chem. 10*, 221−264.
(49) Vreven, T., Mennucci, B., da Silva, C. O., Morokuma, K., and Tomasi, J. (2001) The ONIOM-PCM method: Combining the hybrid molecular orbital method and the polarizable continuum model for solvation. Application to the geometry and properties of a merocyanine in solution. *J. Chem. Phys. 115*, 62−72.
(50) Mo, S. J., Vreven, T., Mennucci, B., Morokuma, K., and Tomasi, J. (2004) Theoretical study of the $S(N)_2$ reaction of Cl-(H_2O)+CH_3Cl using our own N-layered integrated molecular orbital and molecular mechanics polarizable continuum model method (ONIOM-PCM). *Theor. Chem. Acc. 111*, 154−161.
(51) Cerqueira, N. M., Fernandes, P. A., Eriksson, L. A., and Ramos, M. J. (2006) Dehydration of ribonucleotides catalyzed by ribonucleotide reductase: The role of the enzyme. *Biophys. J. 90*, 2109−2119.
(52) Cerqueira, N. M., Fernandes, P. A., Eriksson, L. A., and Ramos, M. J. (2004) Ribonucleotide activation by enzyme ribonucleotide reductase: Understanding the role of the enzyme. *J. Comput. Chem. 25*, 2031−2037.
(53) Carvalho, A. T., Fernandes, P. A., and Ramos, M. J. (2006) Theoretical study of the unusual protonation properties of the active site cysteines in thioredoxin. *J. Phys. Chem. B 110*, 5758−5761.
(54) Carvalho, A. T., Fernandes, P. A., and Ramos, M. J. (2006) Determination of the DeltapKa between the active site cysteines of thioredoxin and DsbA. *J. Comput. Chem. 27*, 966−975.
(55) Dourado, D. F., Fernandes, P. A., Mannervik, B., and Ramos, M. J. (2010) Glutathione transferase A1-1: Catalytic importance of arginine 15. *J. Phys. Chem. B 114*, 1690−1697.
(56) Carvalho, A. T. P., Fernandes, P. A., and Ramos, M. J. (2011) The catalytic mechanism of RNA polymerase II. *J. Chem. Theory Comput. 7*, 1177−1188.
(57) Ramos, M. J., and Fernandes, P. A. (2008) Computational enzymatic catalysis. *Acc. Chem. Res. 41*, 689−698.
(58) Oliveira, E. F., Cerqueira, N. M., Fernandes, P. A., and Ramos, M. J. (2011) Mechanism of formation of the internal aldimine in pyridoxal 5′-phosphate-dependent enzymes. *J. Am. Chem. Soc. 133*, 15496−15505.
(59) Lyttle, M. H., Satyam, A., Hocker, M. D., Bauer, K. E., Caldwell, C. G., Hui, H. C., Morgan, A. S., Mergia, A., and Kauvar, L. M. (1994) Glutathione-S-transferase activates novel alkylating agents. *J. Med. Chem. 37*, 1501−1507.